DEVELOPMENT OF NEURO-FUZZY CONTROLLER FOR A TWO TERMINAL HVDC LINK

Kanungo Barada Mohanty
Department of Electrical Engineering
National Institute of Technology
Rourkela-769008

Abstract: This paper presents the design and development of Neuro-Fuzzy controllers for the dc link current control in a two-terminal HVDC system. The dc link current error and its time derivative have been taken as the two inputs to the controller for deriving the control action, i.e., the firing angle of the converter. The basic structure of a Fuzzy controller has been modified to develop a Neuro-Fuzzy P-D and a Neuro-Fuzzy P-I controller. The simulation results on a benchmark model, show the advantage of the proposed controller.

1. INTRODUCTION

The HVDC (High Voltage DC) system falls into the class of non-linear and non-autonomous plants. The performance of the HVDC system is highly influenced by the current control of the AC/DC converter and extinction angle control of DC/AC inverter. Due to high degree of non-linearity and uncertainty, and non-availability of accurate mathematical description of the HVDC systems, the design of fixed gain PID controllers is difficult. Therefore, to obtain optimum system performance it is essential to go for some advanced control strategies, where the wide variations in the operating points and uncertain system configurations can be taken care. These controllers also need attention for AC system voltage instability. So the design of controllers for this system is a challenging task. A number of HVDC control system design techniques have been reported. Alexandridis and Galanos [1] have proposed a Kalman filter based approach for an optimal current regulator for converter side. To and David [2] have undertaken a systematic investigation of the full potential of using HVDC

link to ensure the stability of operation, and to enhance the performance of the interconnected AC systems. Control system design for HVDC link is also reported in [3].

Recent research on application of knowledge based intelligent techniques to the control problems hints their effectiveness in HVDC links. Changes in environment and performance criteria, unmeasurable disturbances and component failures are some of the characteristics, which necessitate intelligent and knowledge based control. The fuzzy logic controller [4] is one such simple rule-based control system. The main advantage of fuzzy controller is that, it provides an inexpensive solution for controlling ill-known complex systems. Fuzzy controllers are already used in appliances, computer subsystems, industrial systems, automotive-related applications, consumer electronics, and so on. On the other hand, Artificial Neural Networks with its massive parallelism and ability to learn any kind of nonlinear mapping are used to address some of the very practical control problems. A neuro-controller (neural networks based control system) [5] in general, performs a specific form of adaptive control, with the controller taking the form of a

multi-layer network and the adaptable parameters being defined as the adjustable weights. A comparative study of P-I controller and neuro-controller for HVDC system is carried out in [6]. To extract the advantages of both types of controllers, i.e., fuzzy- and neuro-, a combination of both types is devised, which has lead to Neuro-Fuzzy controllers [7-8].

In this work, two types of Neuro-Fuzzy controllers have been developed and tested for their effectiveness on a two-terminal HVDC benchmark model. The conventional P-I controller is completely replaced by these controllers. The Neuro-Fuzzy P-I controller makes use of the dc link current error and its derivative, to derive the incremental firing angle of the converter, so as to maintain the DC link current constant. On the other hand, the Neuro-Fuzzy P-D controller makes use of the same variables to derive the absolute firing angle. In both the cases the on-line training is performed at the output layer, taking the current error as the index. Simulation results show the comparative performance of the proposed controllers with the conventional P-I controller.

2. HVDC SYSTEM MODEL

In last 15 years, a wide variety of HVDC converter control strategies have been tested and optimized with the help of various digital simulation programs. This has led to establishment of an HVDC benchmark model [9]. The normal point-to-point HVDC benchmark model is slightly modified here to provide 6-pulse operation. The filters, transmission line, transformers etc. on either side of the DC link are represented in detail. The HVDC system described in Fig. 1 has the following subsystems.

2.1 Converter End AC System

The converter end (sending end) AC system (3240 MVA, 85 deg.) consists of a constant voltage and constant frequency source behind an L-LR network, which represents the Thevenin's equivalent impedance of the AC network. The short circuit ratio (SCR) is approximately 14.5 representing a strong system. The impedance network consists of: R = 1.267 Ω, L_1 = 2.735 mH, L_2 = 7.67 mH. Data for the AC filters at the

sending end (138 kV, 178 MVA) are given in Table -1.

Table -1
Data for AC filters at sending end

n	5th	7th	11th
R(Ω)	2.0	3.0	2.0
L(H)	0.0614	0.0614	0.0152
C(μF)	4.58	2.337	3.84

2.2 Inverter End AC System

The inverter end (receiving end) AC system (2200 MVA, 78 deg.) consists of a constant voltage, constant frequency source behind an L-LR network. The short circuit ratio (SCR) is roughly 3.5 representing a relatively weak system. The impedance network consists of: R = 14.2 Ω, L_1 = 27.7 mH, L_2 = 44.3 mH.

The data for the AC filters at the receiving end (138 kV, 178 MVA) are given in Table -2.

Table -2
Data for AC filters at receiving end

n	5th	7th	11th
R(Ω)	8.0	8.0	3.0
L(H)	0.168	0.168	0.0444
C(μF)	1.67	0.852	1.310

2.3 DC Subsystems

Both the inverter end and converter end DC subsystems are identical. Each DC subsystem consists of a large smoothing inductor in series between the power converter and DC transmission line. A 6th harmonic DC filter has been connected in parallel to take care of DC voltage harmonics. Smoothing inductor: L_d = 0.75 H.

Sixth harmonic filter: R=24.0Ω, L=0.2444 H, C=0.8 μF.

2.4 DC Transmission Line

A 556 miles (894 km) long transmission line connects the converter and inverter DC subsystems. The following data pertains to the details of the transmission line:
Steady state low frequency = 5 Hz, Transient high frequency = 90 Hz, Mode traveling time =3.037

ms, Characteristic impedance = 300 Ω, Mode resistance at the low frequency = 0.025 Ω, Mode resistance at the high frequency = 0.03 Ω

In addition to the above four main subsystems, the HVDC system also includes the converter current control and inverter extinction angle control systems. For HVDC control and system fault studies a time-step of 50 μs is customarily chosen. This time-step is slightly more than $1°$ for a 60Hz waveform and can result in generation of non-characteristic harmonics. This difficulty is eliminated if the thyristor switching is interpolated to within a fraction of time step. An electro-magnetic transient simulation program, EMTDC is used for the purpose of simulation. EMTDC is capable of such interpolations. This is also capable of accurately modeling the transmission lines for coupling effects, HVDC converters and transformer saturation non-linearity.

3. DEVELOPMENT OF NEURO-FUZZY CONTROLLER

The structure of the Neuro-Fuzzy controller is shown in Fig. 2. This network structure resembles the Cerebellum Model Articulation Controller (CMAC) architecture [8]. The CMAC neural network is a perceptron-like associative memory with overlapping receptive fields, and uses two maps. The first one maps the input space to the association space, or '*the state space detectors*', which are AND gates with several binary inputs and a binary output. This map explains input generalization. The overlaying sensors are arranged in such a way that each input variable excites exactly **C** input sensors, where, **C** = the generalization factor. The second map connects the association space, or the AND gates to the output space via adjustable weights W_i. This CMAC architecture can be considered as a generalization of a fuzzy controller [4] in the following sense:

- The receptive fields of CMAC can be considered as the membership functions of a fuzzy controller with the constraint that only two receptive fields can be overlaid, i.e., the generalization factor **C** = 2.
- The AND gate of CMAC, is the generalization of the Zadeh AND gate in the fuzzy controller.

With the above remarks, the first map of CMAC is replaced by a fuzzifier. This stage is shown by P, Z, N blocks of Fig. 2. Function of this stage is the same as fuzzification of a fuzzy controller to compute the degree of membership (μ_i) of the input in each fuzzy subset (P, Z, N). The second map of CMAC is a generalization of the inference engine of a fuzzy controller. In inference engine of a fuzzy controller, a Zadeh AND operation is performed corresponding to each rule. In the second stage of this novel controller, each Zadeh AND block is excited by **C** = 2 (the generalization factor) number of inputs (μ_i) and is associated with a weight layer W_i. The weight layer is similar to neuron weights, and is adapted to tune the controller for a specific system. The weighted output of this controller is given by:

$$y = out = \frac{\sum \mu_i * W_i}{\sum \mu_i} \qquad (1)$$

This controller is a hybrid of CMAC neural controller and fuzzy controller. Hence it can be termed as a Neuro-Fuzzy controller. The principle for on-line adjustment of the weights is to minimize the square of the difference between the desired output (y_d) and actual output (y), i.e.,

$$E = (y_d - y)^2 \qquad (2)$$

The learning law is gradient type and given by eqn. (3).

$$\Delta W_i = -\eta * \frac{\partial E}{\partial W_i} \qquad (3)$$

where, η is a positive constant called the learning coefficient. From eqns. (1-3), in an iterative learning process, the weights change according to eqn. (4).

$$W_i(k+1) = W_i(k) + 2 \eta (y_d - y)\frac{\mu_i}{\sum \mu_i} \qquad (4)$$

This learning process is the typical Bennard-Widrow delta rule.

This Neuro-Fuzzy controller is tested in two forms: (i) Proportional-Integral (P-I) type, (ii) Proportional-Derivative (P-D) type. For converter current control, the crispy inputs to the Neuro-Fuzzy controller are: (i) dc link current error, $\Delta I_{dc} = I_{dcrf} - I_{dc}$, where, I_{dcrf} = reference value of the dc link current, I_{dc} = measured dc link current, and (ii) rate of change of dc link current error, $\Delta \dot{I}_{dc}$. These two inputs are then normalized to per unit

values by corresponding gain factors, g_e and g_r as follows.

$$\text{error} = g_e * \Delta I_{dc}, \quad \text{and} \quad \text{rate} = g_r * \Delta \dot{I}_{dc}$$

The membership functions for these two normalized inputs are shown in Fig. 3. Degree of membership (μ_i) of each normalized input in each fuzzy subset (P, Z, N) are computed by the first stage of mapping, which is the fuzzy controller. Then in the second stage of mapping, the neuro controller computes the network output **out** from the above inputs (output of first stage) through different weights W_i as given by eqn. (1). The final control signal from the controller is the firing angle (α) of the converter. For the Neuro-Fuzzy P-D controller, the firing angle is: $\alpha = g_u * \text{out}$.

For the Neuro-Fuzzy P-I controller, the firing angle at k^{th} sampling instant is: $\alpha(k) = \alpha(k-1) + g_u * \text{out}$

where, g_u = Denormalization Factor (DF)

4. RESULTS AND DISCUSSIONS

To test the effectiveness of the above controllers the HVDC system is subjected to the following types of disturbances.
1. Single-line-to-ground fault at the inverter end AC bus
2. Three-phase-to-ground fault at the converter end AC bus
3. DC-line-to-line fault at the inverter end

4.1. Single-line-to-ground fault at the inverter end AC bus

A single-line-to-ground fault has been simulated in the inverter end AC system for about 5-cycles. The inverter end AC system is weaker than that of converter end with an SCR of around 3.5. Therefore such kind of faults result in sudden voltage collapse on all the other phases leading to commutation failures and other difficulties in the converter operation. This also leads to unbalanced operation of the converter even after the fault is cleared. The inverter DC voltage plots shown in Fig. 4 indicate a number of commutation failures of the corresponding thyristors. The firing instants are now uncertain and hence the inverter extinction angle (γ) controller loses control over the DC link current recovery. The converter current regulator mostly influences the transient performance under this condition. Therefore, the comparative study shows substantial difference in the system response for different types of controllers. From the above comparison it is apparent that:
- The conventional P-I regulator is inferior to others.
- The Neuro-Fuzzy P-D controller exhibits best performance in terms of the transient recovery, as the damping is much faster.

4.2. Three-phase-to-ground fault at the converter end AC bus

Variation of dc link voltage and current, and converter firing angle due to a three-phase-to-ground fault at the rectifier end AC bus are shown in Fig. 5. The dc bus voltage completely collapses and results in commutation failure of the converter thyristors. During the fault, the DC link current drops to zero and the firing angle settles at the minimum value. The zero current and zero power condition lead to complete de-energization of the DC link. As soon as the fault is cleared the converter current controller gets activated, and it is in this period when the performance is influenced by the controller actions. From the comparative study presented the following facts are apparent.
- The current controller is almost defunct as the firing angle hits the minimum limit. It is activated only when the fault is cleared. Therefore much difference is not observed in the responses resulting from various controller actions.
- Responses resulting from the Neuro-Fuzzy P-D controller show the least amount of oscillations as compared to other controllers.

4.3. DC-line-to-line fault at the inverter end

Fig. 6 shows the responses due to a 5-cycle DC-line-to-line fault at the inverter end. This kind of fault is the severest fault when the connected AC system is weak. The nature of the fault is balanced but most critical due to the low SCR of the inverter end AC system. This is in a way similar to a 3-phase fault at the inverter bus, since the total power injection becomes zero. The DC power oscillations may give rise to uncontrolled dv/dt and di/dt stress on the converter thyristors. Also the oscillations in the inverter AC bus voltage may be detrimental to the loads at the inverter end. As seen from the

figures the conventional P-I controller makes the system oscillate even after the fault is removed. In this case, since the current error becomes high, firing angle of the converter hits the maximum limit. Consequently the current regulator becomes temporarily ineffective. From the comparative results it may be concluded that:

- The DC link behavior is primarily decided by the action of the extinction angle controller rather than the converter current regulator.
- The oscillations have been minimized in case of the Neuro-Fuzzy P-D controller.

5. CONCLUSIONS

The performance of a point-to-point HVDC link is studied under the action of Neuro-Fuzzy controllers. Due to the non-availability of a standard design technique for the Neuro-Fuzzy controller, the control parameters are determined by trial and error method.

From the simulation studies the following general conclusions are drawn.

1. The converter side AC system being stronger recovers very fast, after any type of disturbance, overriding the effect of most of the controller actions. Therefore, for any type of fault on the converter AC or DC bus, much difference is not observed in the current and voltage responses for different controllers.
2. For the faults on the inverter side, the proposed Neuro-Fuzzy P-D controller makes the system recover much faster than the conventional P-I controller. The Neuro-Fuzzy P-I controller performs in between the Neuro-Fuzzy P-D and conventional P-I controllers.

The application of the linguistic rules is very simple. The implementation of Fuzzy and Neuro-Fuzzy controllers is also less complicated than that of sophisticated identification and optimization procedures. The results obtained display the superiority of Neuro-Fuzzy controllers over the P-I type.

REFERENCES

1. A. T. Alexandridis, and G. D. Galanos, "Design of an optimal current regulator for weak AC/DC systems using Kalman filtering in the presence of unknown inputs", Proc. of IEE, pt. C, Vol. 136, No. 2, pp. 57-63, Mar. 1989.
2. K. W. V. To, and A. K. David, "Using an HVDC link to control the behavior of generators", Proc. of International Power Engineering Conference, Singapore, Mar. 1993, pp. 205-209.
3. N. Rostamkolai, C. A. Wegner, R. J. Piwko, et al, "Control design of Santo Tome back-to-back HVDC link", IEEE Trans. on Power Systems, Vol. 8, No. 3, pp. 1250-1256, Aug. 1992.
4. C. C. Lee, "Fuzzy logic in control systems: fuzzy logic controller, part-I", IEEE Trans. on Systems, Man and Cybernets, Vol. 20, No. 2, pp. 404-418, Mar/Apr 1990
5. A. G. Barto, *Neural Networks for Control*, MIT Press, Cambridge, 1990.
6. V. K. Sood, N. Kandil, R. V. Patel, and K. Khorasani, "Comparative evaluation of neural network-based and PI controllers for HVDC transmission", IEEE Trans. Power Electrn, Vol. 9, No. 2, pp. 208-215, May 1994.
7. J. Shing, and R. Jang, "ANFIS: Adaptive Network based Fuzzy Inference System", IEEE Trans. on Systems Man and Cybernatics, Vol. 23, No. 3, pp. 665-690, May/June 1993.
8. G. Calcev, "A self tuning Neuro-Fuzzy controller", Proc. of Int. Symp. on Intelligent Control, Chicago, USA, Aug. 1993, pp. 577-581.
9. M. Szechtman et al, "First benchmark model for HVDC control studies", Electra, No.135, pp. 54-67, Apr. 1991.
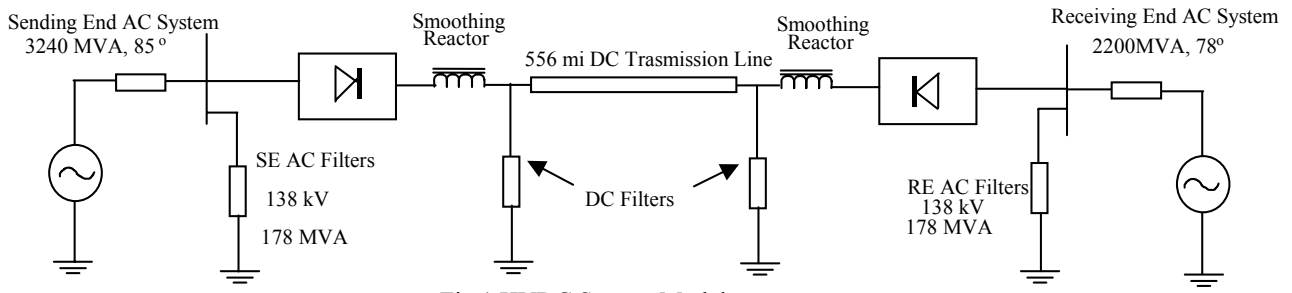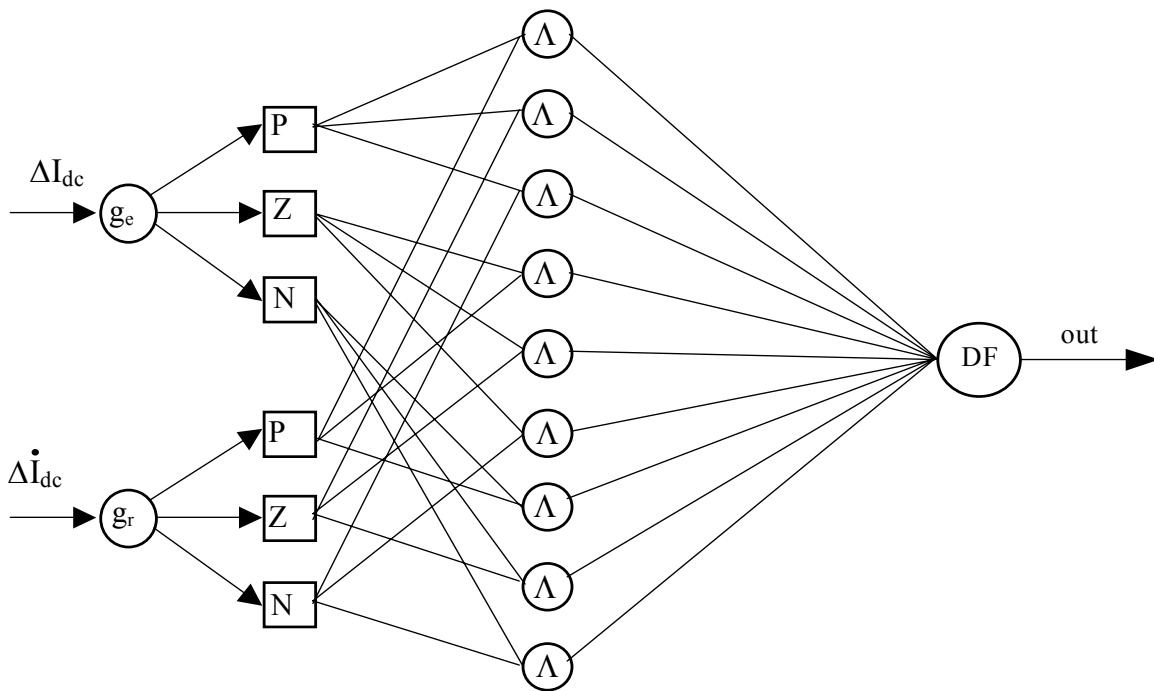
Sending End AC System
3240 MVA, 85 °

Smoothing
Reactor

556 mi DC Trasmission Line

Smoothing
Reactor

Receiving End AC System
2200MVA, 78º

SE AC Filters
138 kV
178 MVA

DC Filters

RE AC Filters
138 kV
178 MVA

Fig.1 HVDC System Model

ΔI_{dc}

g_e

P
Z
N

$\Delta \dot{I}_{dc}$

g_r

P
Z
N

DF

out

Λ - AND Blocks with adjustable weight;   P, Z, N- Positive, Zero, Negative Input Fuzzy sets
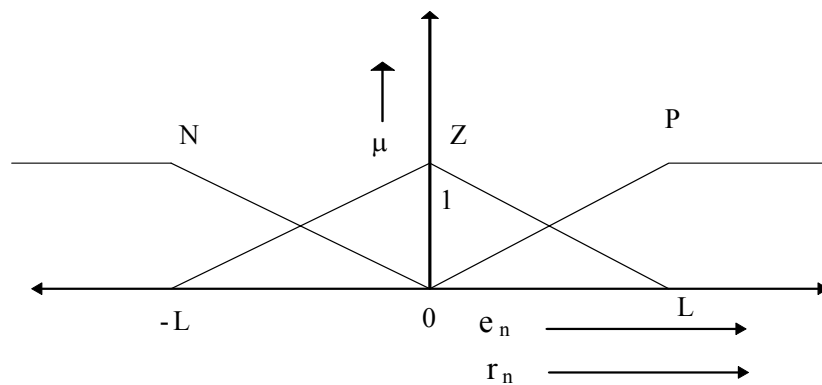
Fig. 2 The Neuro-Fuzzy Controller

N
μ
Z
P
1
-L
0
e_n
L
r_n

Fig. 3 Membership functions for normalized error and normalized rate of change in error

13

Conventional P-I   **Neuro-Fuzzy P-I**   **Neuro-Fuzzy P-D**

Fig. 4 Single-line-to-ground fault at the inverter end AC bus

Conventional P-I   **Neuro-Fuzzy P-I**   **Neuro-Fuzzy P-D**
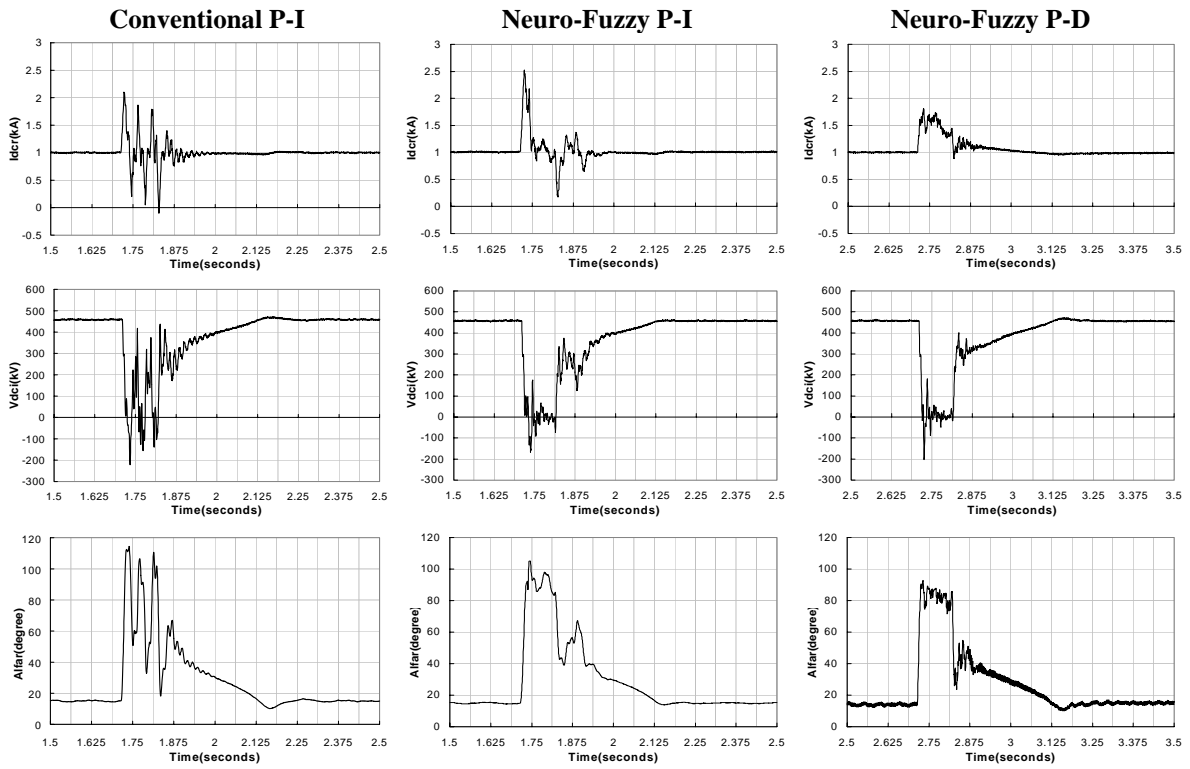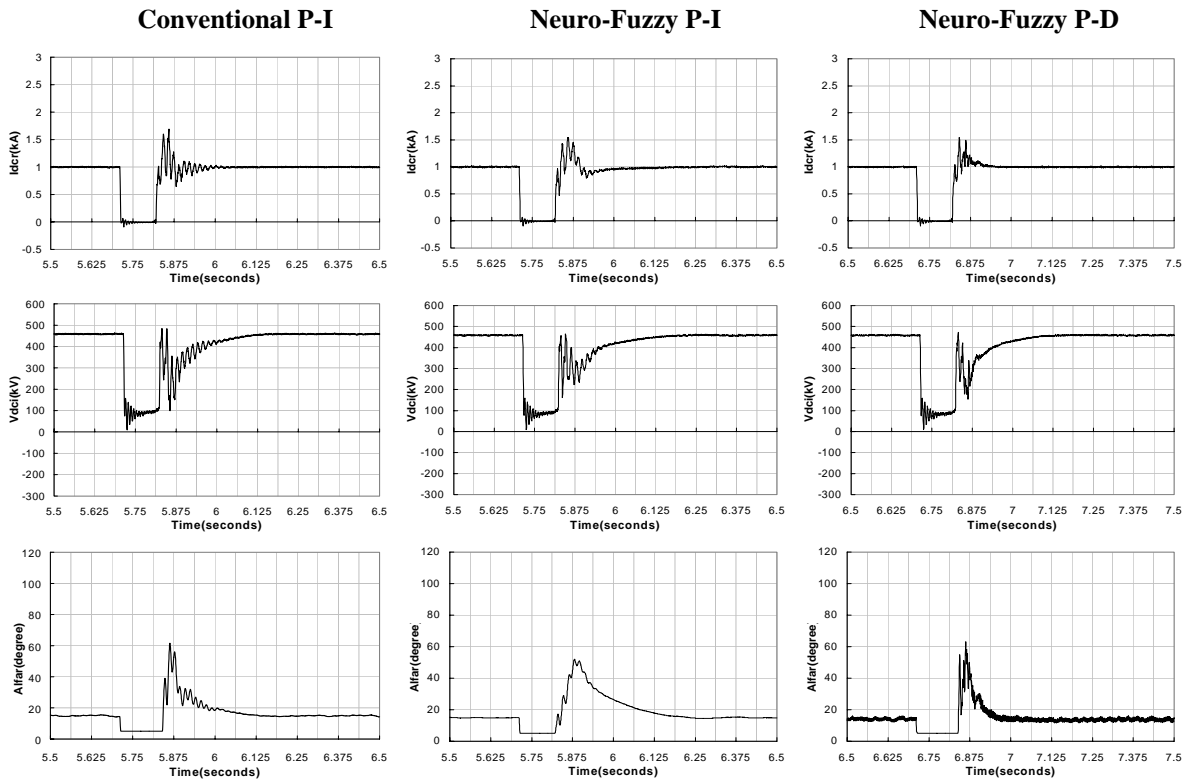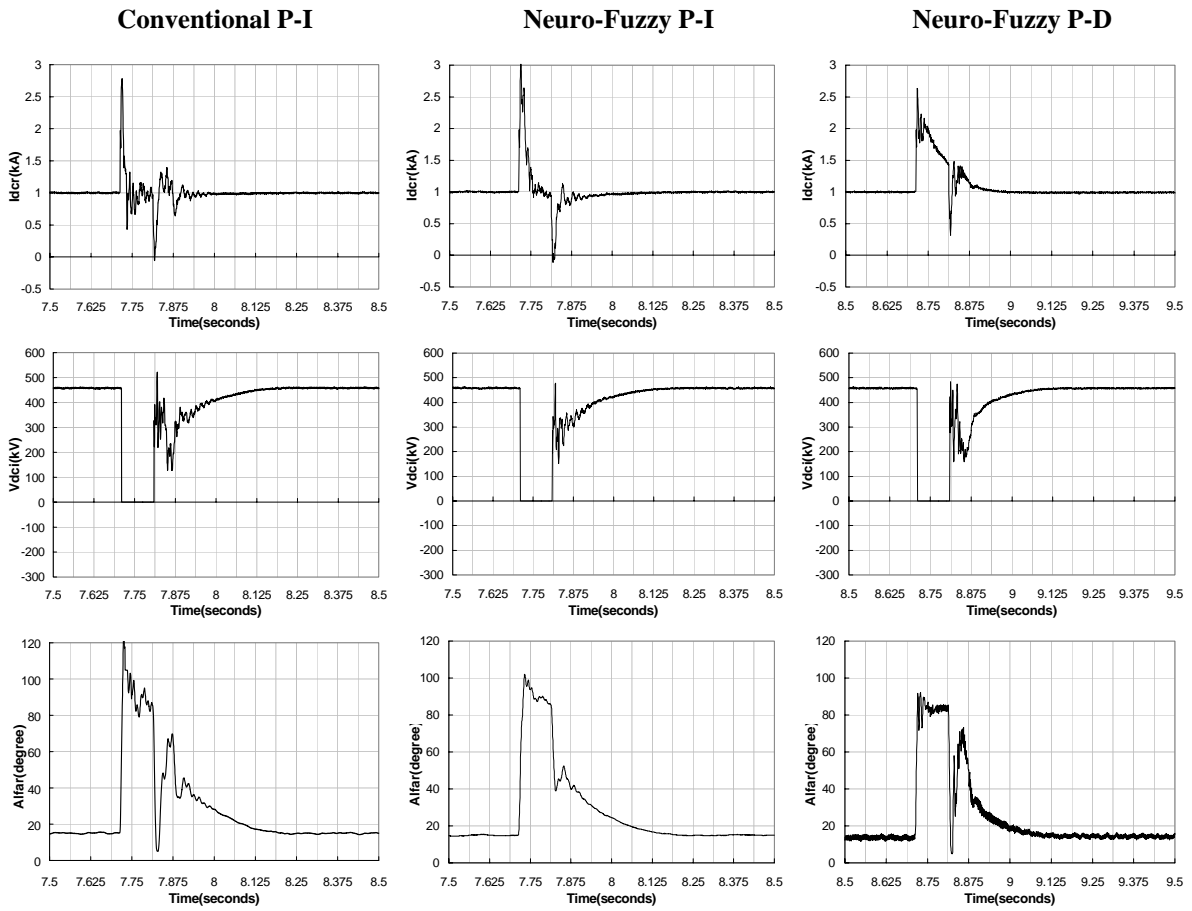
Fig. 5 Three-phase-to-ground fault at the rectifier end AC bus

Fig. 6 DC line-to-line fault at the inverter end